IOP PUBLISHING PHYSICA SCRIPTA

Phys. Scr. **79** (2009) 065301 (13pp) doi:10.1088/0031-8949/79/06/065301

Multireference Møller–Plesset perturbation theory results on levels and transition rates in Al-like ions of iron group elements

Juan A Santana[1], **Yasuyuki Ishikawa**[1] **and Elmar Träbert**[2,3]

[1] Department of Chemistry and the Chemical Physics Program, University of Puerto Rico, PO Box 23346, San Juan, Puerto Rico 00931-3346, USA
[2] Astronomisches Institut, Ruhr-Universität Bochum, D-44780 Bochum, Germany
[3] Physics Division, LLNL, PO Box 808, Livermore, CA 94551, USA

E-mail: yishikawa@uprrp.edu and traebert@astro.rub.de

Received 27 November 2008
Accepted for publication 22 April 2009
Published 22 May 2009
Online at stacks.iop.org/PhysScr/79/065301

Abstract
Ground configuration and low-lying levels of Al-like ions contribute to a variety of laboratory and solar spectra, but the available information in databases are neither complete nor necessarily correct. We have performed multireference Møller–Plesset perturbation theory calculations that approach spectroscopic accuracy in order to check the information that databases hold on the 40 lowest levels of Al-like ions of iron group elements (K through Ge), and to provide input for the interpretation of concurrent experiments. Our results indicate problems of the database holdings on the levels of the lowest quartet levels in the lighter elements of the range studied. The results of our calculations of the decay rates of five long-lived levels ($3s^2 3p\,^2P^o_{3/2}$, $3s3p^2\,^4P^o_J$ and $3s3p3d\,^4F^o_{9/2}$) are compared with lifetime data from beam-foil, electron beam ion trap and heavy-ion storage ring experiments.

PACS numbers: 32.70.Cs, 31.15.am, 34.50.Fa

(Some figures in this article are in colour only in the electronic version.)

1. Introduction

Ions with a single electron outside of closed shells have been of high interest for spectroscopy because of their prominent resonance lines and for theory because of their perceived simplicity. Detailed studies over the past decades have revealed how complex the role of the inner electronic shells and their virtual excitations can be. Nevertheless, high accuracy has been achieved in both spectroscopy (Li-, Na- and Cu-like ions up to uranium ($Z = 92$)) and many-body perturbation theory calculations [1, 2]. A second electron in the valence shell introduces massive complications; while experiment can reach the same accuracy as for one-electron spectra, theory has been struggling. Calculations of Al-like ions sometimes have been extensive, but have covered only a single element at a time [3–15], while others sometimes employed rather few configurations when tabulating results for a full isoelectronic sequence. For calculations of a sequence of ions along the Al sequence, see, for example [16–22]. These calculations use different approximations and historically reflect the growing availability of computing resources. Some of the calculations listed are limited to electric dipole (M1) transitions, others include higher multipole order radiation, but only within a set of levels of limited total angular momentum J that can connect to the ground configuration by E1 radiation. (These citations of theoretical work as well as the ones for experimental data below represent typical samples, but are certainly incomplete; for example, Wei *et al* [23] have calculated $n = 3$–4 transitions in various ions, but these transitions play no role in the present discussion.) Beyond the lowest charge state ions of the Al sequence, the experimental

 © 2009 The Royal Swedish Academy of Sciences Printed in the UK

database has been growing in bursts, whenever specific techniques or devices (beam foil spectroscopy, laser-produced plasmas and tokamaks) gave access to a new range of charge states or observation options [24–45]. Several attempts have been made to compare calculated results and measurements with the aim of establishing isoelectronic trends that would be useful for interpolation or extrapolation to ion species not directly covered, often introducing semiempirical corrections to the calculations [46, 47]. These attempts usually were limited to a sample of levels, for example to the $3s3p^2$ quartet term and its intercombination decays, or the $3s3p3d\,^4F^o_J$ levels some of which are exceptionally long-lived [8, 48, 49].

The quality of the experimental data hinges on the observation conditions. While the resonance lines are easily excited, the population of long-lived levels often depends on the particle density in the light source; very long-lived levels may be quenched by collisions. In beam-foil spectroscopy, the emission from long-lived levels is spread out so much that the observed signal rate per unit length of ion beam may be extremely low, and ultimately too low to be significant. In that case, a low-density plasma such as is available in an electron beam ion trap (EBIT) may be the laboratory light source of choice for measurements of electric-dipole (E1) forbidden transitions. Near the low end of the isoelectronic sequence, levels that have spin-changing transition decay channels only (the intercombination decays of the $3s3p^2\,^4P_J$ levels) also have very long lifetimes. Consequently, for many elements in that range the positions of the quartet levels have not been established from direct observations of their decays to the ground state, but indirectly via chains of other transitions. Therefore inconsistencies of the tabulated level energies are to be expected more in this range than in others.

Many atomic structure calculations are guided by the Hartree–Fock approach. In the 1930s, Møller and Plesset [50] developed another approximation, which to zero order corresponds to the Hartree–Fock solution, but with significant extensions to second order that promise higher accuracy. Very recently our multireference Møller–Plesset (MR-MP) perturbation theory approach has reached an accuracy comparable with that of recent measurements of Zn-like ions (two valence electrons) at EBITs [51]. A third electron in the valence shell is expected to cause even more problems for calculations, especially if the first two of these electrons are no more locked in a ns^2 configuration, but possibly excited. However, recent calculations by our technique of the fine structure splitting and M1 transition rate of the $3s^23p\,^2P^o$ ground term of Al-like Fe ($Z = 26$) have reproduced the spectroscopically known interval and the transition rate [52] without any need for a 'semiempirical' correction. From this success we take encouragement to extend the calculations to all levels up to the 3s3p3d configuration of Al-like ions of iron group elements from potassium (K, $Z = 19$) to germanium (Ge, $Z = 32$). The resonance and intercombination lines of these elements have partly been seen in a variety of light sources, from laser-produced plasmas, foil-excited ion beams and ion clouds in EBITs to the solar corona. Because of the different particle densities in such light sources, the level populations differ drastically, and line intensities may be exploited for plasma diagnostics. The diagnostics usually involve radiative-collisional modeling, which depends rather crucially on the level lifetimes of the more long-lived levels (with radiative decay rates of the same order of magnitude as the collision rates). For this reason, we also present lifetime results for five long-lived levels among the lowest 40 levels, and compare our results with the energy level holdings of databases [40, 53] and to the results of lifetime measurements.

2. Computational details

Levels and level lifetimes of Al-like ions have been computed by a variety of techniques before, employing nonrelativistic and relativistic techniques (see, for example [6, 16–18, 20–22]). Among those studies, Huang [18] has covered the elements up to $Z = 92$, but used a rather small number of configurations in multiconfiguration Dirac–Fock (MCDF) calculations. The observation along the isoelectronic sequence of line intensity anomalies due to level mixing underlines the need for detail in the description of Al-like ions [54]. Gupta and Msezane have treated a selection of elements using the CIV3 code with a large number of configurations [4, 5, 7–12, 15]. Compared with all such earlier works, we expect higher accuracy than has been available before, and that from *ab initio* calculations, in contrast to earlier calculations (like those by Fawcett [17] who used a version of the Hartree XR Cowan code [55]) that involved the scaling of parameters to match the experimental level structure. Such scaled calculations are very helpful for interpolating (and slightly extrapolating) experimental data in practical applications. However, when judging the quality and consistency of experimental data sets, *ab initio* calculations have the advantage of results that are not biased by human interference, but may be less close to experimental findings. The goal of modeling the atomic structure is of course to achieve agreement with experimental findings without taking recourse to semi-empirical corrections.

Theoretical background information and computational details of the combined state-averaged MCDF Self-Consistent Field (SCF) plus the state-specific MR-MP method, as well as a number of theoretical transition probabilities have been presented elsewhere [51, 52, 56–62]. Essentially, the method consists of three basic steps. The process begins with a state-average MCDF-Breit (MCDFB) SCF calculation for the ground and low-lying excited states of the ion, to obtain a common set of core and valence spinors in the V^N potential. This is followed by a relativistic multireference Configuration Interaction (CI) procedure [63], including the calculation of highly excited states, in order to account for near-degeneracy effects or strong configuration mixing among the excited states. The relativistic CI, however, fails to account for the bulk of dynamic correlation among all levels unless a very larger number of configurations, of the order of 1×10^6, are included in the CI calculations. The residual dynamic correlation corrections, however, can easily be accounted for by state-specific MR-MP calculations based on the CI wavefunctions. In this section, we briefly outline the computational details to calculate the energy terms and transition probabilities for the aluminium isoelectronic sequence from K^{+6} to Ge^{+19}.

The large and small radial components of the bound Dirac spinors were expanded in sets of even-tempered

Gaussian-type functions (GTF) that satisfy the boundary conditions associated with the finite nucleus [64] and are automatically kinetically balanced [65]. The speed of light is taken to be 137.0359895 a.u. throughout this study. For all the systems investigated, even-tempered basis sets of 26s24p22d20f18g18h Gaussian spinors for up to angular momentum $L = 5$ and 15 Gaussian spinors for $L = 6$–11 are employed. The order of the partial-wave expansion $L_{\max}$, the highest angular momentum of the spinors included in the virtual space, is $L_{\max} = 11$ throughout this study. The nuclei were simulated as spheres of uniform proton charge with the radii (Bohr) $R = 2.2677 \times 10^{-5}\, A^{1/3}$, where A(amu) is the atomic mass number.

The state-average MCDFB SCF calculations for the ground and low-lying excited $J = \frac{1}{2} - \frac{5}{2}$ states in Al-like ions were carried out including seven even- and odd-parity Configuration State Functions (CSFs) arising from the $3s^2 3p^1$, $3s^1 3p^2$, $3p^3$ and $3s^2 3d^1$ configurations. Subsequent relativistic CI includes all the CFSs arising from the configurations $3s^m 3p^n 3d^p$ with $m + n + p = 3$ (complete active space of the $n = 3$ manifold) to ensure that the $n = 3$ eigenstates of the matrix CI equation are the upper bounds to the exact Dirac–Coulomb–Breit (DCB) energies. A total of 145 CSFs of $J = \frac{1}{2} - \frac{9}{2}$, 72 even-parity and 73 odd-parity CSFs thus produced, were included in the CI calculations. Subsequently, each of the 145 eigenstates was subjected to state-specific MR-MP refinement to account for the residual dynamic correlation. All electrons have been included in the MR-MP perturbation theory calculation to determine accurately the effects of relativity on electron correlation. Radiative corrections, the Lamb shifts, were estimated for each state by evaluating the electron self-energy and vacuum polarization following an approximation scheme discussed by Indelicato *et al* [66].

MR-MP calculations of electric multipole transition probabilities in the Babushkin and Coulomb gauge have been discussed in more detail in an earlier study [52]. Because of the strong coupling between the large and small components of the Dirac 4-spinors in the electric multipole transition matrix elements, the transition probability evaluated by excluding the negative-energy space in the Coulomb gauge is inaccurate and deviates from the value evaluated in the Babushkin gauge. When contributions from the negative-energy space are included, transition probabilities evaluated in the Coulomb gauge approach those evaluated in the Babushkin gauge. In the present study, electric dipole transition probabilities were evaluated in the Babushkin and Coulomb gauges including negative-energies following the method given in [52].

The calculations have yielded many more results, especially on transition rates, than are to be presented here. A formal presentation of more of the transition rate and lifetime results is under consideration. Until then, more of the results are available upon request from the senior theory coauthor (YI).

3. Levels

The results of our calculations of the lowest 40 energy levels of Al-like ions of K through Ge are listed in tables 1–14. We compare our level values with the data found in the NIST online database [53], because this reflects the experimental knowledge and the varying degree of completeness of information on Al-like ions of various elements. For K, Ca, Sc, Cu, Zn and Ga the NIST database holdings are rather slim, for Ti through Ni the data collection is almost complete (for the first 40 levels in Al-like ions), and for Ge it is somewhere in the middle. The difference between the NIST listed values and our calculational results is typically much below 0.05% (often better than 0.02%) for the levels in the more completely known spectra. The deviations are clearly larger for many (not all) of the levels in the incompletely known spectra. This scatter suggests that the 'known' data are not just incomplete, but also of lesser quality. Examples are the $3s3p^2$ quartet levels

Table 1. Comparison of second-order MR-MP calculated energies (in cm^{-1}) and NIST experimental values in K^{6+}.

Configuration	Level	MR-MP	NIST	Deviation (per cent)
$3s^2 3p$	$^2P^o_{1/2}$	0	0	0
	$^2P^o_{3/2}$	3135	3134	−0.032
$3s3p^2$	$^4P_{1/2}$	114845	114650	−0.170
	$^4P_{3/2}$	115988	115786	−0.174
	$^4P_{5/2}$	117726	117523	−0.173
	$^2D_{3/2}$	151859	151883.9	0.016
	$^2D_{5/2}$	152028	152051.7	0.016
	$^2S_{1/2}$	193146	193084.5	−0.032
	$^2P_{1/2}$	206554	206502.9	−0.025
	$^2P_{3/2}$	208484	208432.5	−0.025
$3s^2 3d$	$^2D_{3/2}$	250943	250663	−0.112
	$^2D_{5/2}$	251070	250781	−0.115
$3p^3$	$^2D^o_{3/2}$	297753		
	$^2D^o_{5/2}$	298062		
	$^4S^o_{3/2}$	307968	307777	−0.062
	$^2P^o_{1/2}$	335349		
	$^2P^o_{3/2}$	335380		
$3s3p[^3P]3d$	$^4F^o_{3/2}$	334167		
	$^4F^o_{5/2}$	334811		
	$^4F^o_{7/2}$	335734		
	$^4F^o_{9/2}$	336959		
	$^4P^o_{5/2}$	362840	362492	−0.096
	$^4D^o_{3/2}$	363682	363321	−0.099
	$^4D^o_{1/2}$	364381		
	$^4P^o_{1/2}$	366070	365688	−0.104
	$^4P^o_{3/2}$	366476	366101	−0.102
	$^4D^o_{5/2}$	366811	366409	−0.110
	$^4D^o_{7/2}$	366978	366556	−0.115
	$^4D^o_{5/2}$	376542		
	$^4D^o_{3/2}$	376571		
	$^4F^o_{5/2}$	394592		
	$^4P^o_{7/2}$	397091		
	$^4P^o_{3/2}$	431251		
	$^4P^o_{1/2}$	432181		
$3s3p[^1P]3d$	$^4F^o_{7/2}$	432891		
	$^4F^o_{5/2}$	433529		
	$^4P^o_{1/2}$	447334		
	$^4D^o_{3/2}$	447478		
	$^4P^o_{3/2}$	451899		
	$^4D^o_{5/2}$	452353		

Table 2. Comparison of second-order MR-MP calculated energies (in cm^{-1}) and NIST experimental values in Ca^{7+}.

Configuration	Level	MR-MP	NIST	Deviation (per cent)
$3s^23p$	$^2P^o_{1/2}$	0	0	0
	$^2P^o_{3/2}$	4307	4308.3	0.030
$3s3p^2$	$^4P_{1/2}$	129796	129100	−0.539
	$^4P_{3/2}$	131382	130678	−0.539
	$^4P_{5/2}$	133745	133042	−0.528
	$^2D_{3/2}$	171537	171572.2	0.021
	$^2D_{5/2}$	171789	171830.7	0.024
	$^2S_{1/2}$	216548	216584.9	0.017
	$^2P_{1/2}$	231037	231016.3	−0.009
	$^2P_{3/2}$	233614	233592.8	−0.009
$3s^23d$	$^2D_{3/2}$	282539	282356	−0.065
	$^2D_{5/2}$	282765	282577	0.067
$3p^3$	$^2D^o_{3/2}$	335800		
	$^2D^o_{5/2}$	336255		
	$^4S^o_{3/2}$	345942	345274	−0.193
	$^2P^o_{1/2}$	376944		
	$^2P^o_{3/2}$	377077		
$3s3p[^3P]3d$	$^4F^o_{3/2}$	377423		
	$^4F^o_{5/2}$	378315		
	$^4F^o_{7/2}$	379596		
	$^4F^o_{9/2}$	381304		
	$^4P^o_{5/2}$	409030	408227	−0.197
	$^4D^o_{3/2}$	410107	409291	−0.199
	$^4D^o_{1/2}$	411080	411816	0.179
	$^4P^o_{1/2}$	412581		
	$^4P^o_{3/2}$	413178	412388	−0.192
	$^4D^o_{5/2}$	413592	412772	−0.199
	$^4D^o_{7/2}$	413742	412881	−0.209
	$^4D^o_{5/2}$	423788		
	$^4D^o_{3/2}$	423802		
	$^4F^o_{5/2}$	444185		
	$^4P^o_{7/2}$	447611		
	$^4P^o_{3/2}$	484543		
	$^4P^o_{1/2}$	485933		
$3s3p[^1P]3d$	$^4F^o_{7/2}$	487088		
	$^4F^o_{5/2}$	487944		
	$^4P^o_{1/2}$	502416		
	$^4D^o_{3/2}$	502700		
	$^4P^o_{3/2}$	506781		
	$^4D^o_{5/2}$	507392		

Table 3. Comparison of second-order MR-MP calculated energies (in cm^{-1}) and NIST experimental values in Sc^{7+}.

Configuration	Level	MR-MP	NIST	Deviation (per cent)
$3s^23p$	$^2P^o_{1/2}$	0	0	0
	$^2P^o_{3/2}$	5764	5761.1	−0.050
$3s3p^2$	$^4P_{1/2}$	144970	143500	−1.024
	$^4P_{3/2}$	147118	145622	−1.027
	$^4P_{5/2}$	150249	148779	−0.988
	$^2D_{3/2}$	191573	191609.3	0.019
	$^2D_{5/2}$	191946	191987.1	0.021
	$^2S_{1/2}$	240433	240361.4	−0.030
	$^2P_{1/2}$	255853	255829.4	−0.009
	$^2P_{3/2}$	259180	259153.7	−0.010
$3s^23d$	$^2D_{3/2}$	313992	313860	−0.042
	$^2D_{5/2}$	314357	314214	0.046
$3p^3$	$^2D^o_{3/2}$	374303		
	$^2D^o_{5/2}$	374966		
	$^4S^o_{3/2}$	384478	383047	−0.374
	$^2P^o_{1/2}$	419256		
	$^2P^o_{3/2}$	419568		
$3s3p[^3P]3d$	$^4F^o_{3/2}$	420737		
	$^4F^o_{5/2}$	421944		
	$^4F^o_{7/2}$	423676		
	$^4F^o_{9/2}$	426000		
	$^4P^o_{5/2}$	455201		
	$^4D^o_{3/2}$	456505		
	$^4D^o_{1/2}$	457719		
	$^4P^o_{1/2}$	459344		
	$^4P^o_{3/2}$	460090		
	$^4D^o_{5/2}$	460545		
	$^4D^o_{7/2}$	460636		
	$^4D^o_{3/2}$	471276		
	$^4D^o_{5/2}$	471294		
	$^4F^o_{5/2}$	493692		
	$^4P^o_{7/2}$	498272		
	$^4P^o_{3/2}$	537741		
	$^4P^o_{1/2}$	539716		
$3s3p[^1P]3d$	$^4F^o_{7/2}$	541243		
	$^4F^o_{5/2}$	542357		
	$^4P^o_{1/2}$	557502		
	$^4D^o_{3/2}$	558022		
	$^4P^o_{3/2}$	561660		
	$^4D^o_{5/2}$	562455		

in K, Ca, Sc (with a 1% deviation), the 3s3p3d quartet levels in K, Ca, Cu and Ge (and no data for Zn and Ga), and the $3p^3\,^4S_{3/2}$ level in Ca and Sc. Two significant deviations for $3s3p[^3P]3d$ levels of Cu clearly point to misidentifications.

For the first few elements of our selection, the calculations yield energy levels that are mostly slightly higher than listed in the NIST tables. For the middle of the iron group element sequence, such a slight deviation is only apparent for the highest configuration discussed here. Overall, the systematic deviations are much smaller than for any other published calculation and practically vanishing for elements near Fe.

Seeing the excellent agreement of experimental and calculated energy levels in the elements from Ti through Ni, it appears as a straightforward suggestion that where experimental data are missing, our results can serve as a valid guide. The systematics moreover indicate the aforementioned cases of doubt about the accuracy of some of the listed experimental level data; using our calculational results instead should be a safe bet.

4. Lifetimes

In the Al-like ions of the iron group elements, five excited levels are much longer lived (by roughly two to eight orders of magnitude) than the others. These levels are the upper fine structure level of the ground term, $3s^23p\,^2P^o_{3/2}$ (decaying by M1 and a very weak E2 transition), the three lowest quartet levels, $3s3p^2\,^4P_{1/2,3/2,5/2}$ (decaying by spin-changing E1 transitions) and the $3s3p3d\,^4F^o_{9/2}$ level (with E1-forbidden

Table 4. Comparison of second-order MR-MP calculated energies (in cm^{-1}) and NIST experimental values in Ti^{9+}.

Configuration	Level	MR-MP	NIST	Deviation (per cent)
$3s^23p$	$^2P^o_{1/2}$	0	0	0
	$^2P^o_{3/2}$	7543	7544	0.013
$3s3p^2$	$^4P_{1/2}$	160412	160409	−0.002
	$^4P_{3/2}$	163265	163257	−0.005
	$^4P_{5/2}$	167320	167309	−0.007
	$^2D_{3/2}$	212025	212053	0.013
	$^2D_{5/2}$	212574	212608	0.016
	$^2S_{1/2}$	264594	264456	−0.052
	$^2P_{1/2}$	281072	281051	−0.007
	$^2P_{3/2}$	285238	285220	−0.006
$3s^23d$	$^2D_{3/2}$	345411	345315	−0.028
	$^2D_{5/2}$	345963	345859	−0.030
$3p^3$	$^2D^o_{3/2}$	413358	413397	0.009
	$^2D^o_{5/2}$	414317	414365	0.012
	$^4S^o_{3/2}$	423669	423713	0.010
	$^2P^o_{1/2}$	462184	462142	−0.009
	$^2P^o_{3/2}$	462767	462709	−0.013
$3s3p[^3P]3d$	$^4F^o_{3/2}$	464235		
	$^4F^o_{5/2}$	465834	465910	0.016
	$^4F^o_{7/2}$	468125	468204	0.017
	$^4F^o_{9/2}$	471220	471285	0.014
	$^4P^o_{5/2}$	501506	501474	−0.006
	$^4D^o_{3/2}$	503018	502940	−0.016
	$^4D^o_{1/2}$	504332	504163	−0.034
	$^4P^o_{1/2}$	506701	506849	0.029
	$^4P^o_{3/2}$	507443	507492	0.010
	$^4D^o_{7/2}$	507871	507815	−0.011
	$^4D^o_{5/2}$	507884	507859	−0.005
	$^4D^o_{3/2}$	519127	519034	−0.018
	$^4D^o_{5/2}$	519198	519113	−0.016
	$^4F^o_{5/2}$	543235	543166	−0.013
	$^4P^o_{7/2}$	549227	549148	−0.014
	$^4P^o_{3/2}$	590926	590439	−0.082
	$^4P^o_{1/2}$	593650	593151	−0.084
$3s3p[^1P]3d$	$^4F^o_{7/2}$	595519	595023	0.083
	$^4F^o_{5/2}$	596931	596470	−0.077
	$^4P^o_{1/2}$	612842	612628	−0.035
	$^4D^o_{3/2}$	613542	613252	−0.047
	$^4P^o_{3/2}$	616710	616264	−0.072
	$^4D^o_{5/2}$	617699	617188	−0.083

Table 5. Comparison of second-order MR-MP calculated energies (in cm^{-1}) and NIST experimental values in V^{10+}.

Configuration	Level	MR-MP	NIST	Deviation (per cent)
$3s^23p$	$^2P^o_{1/2}$	0	0	0
	$^2P^o_{3/2}$	9694	9696	0.021
$3s3p^2$	$^4P_{1/2}$	176107	176117	0.006
	$^4P_{3/2}$	179836	179839	0.002
	$^4P_{5/2}$	184987	184992	0.003
	$^2D_{3/2}$	232943	232972	0.012
	$^2D_{5/2}$	233738	233778	0.017
	$^2S_{1/2}$	288991	288914	−0.027
	$^2P_{1/2}$	306803	306801	−0.001
	$^2P_{3/2}$	311892	311890	−0.001
$3s^23d$	$^2D_{3/2}$	376922	376897	−0.007
	$^2D_{5/2}$	377722	377650	−0.019
$3p^3$	$^2D^o_{3/2}$	453014	453057	0.009
	$^2D^o_{5/2}$	454387	454448	0.013
	$^4S^o_{3/2}$	463584	463653	0.015
	$^2P^o_{1/2}$	505716	505765	0.010
	$^2P^o_{3/2}$	506716	506695	−0.004
$3s3p[^3P]3d$	$^4F^o_{3/2}$	507982		
	$^4F^o_{5/2}$	510059	510204	0.028
	$^4F^o_{7/2}$	513033	513127	0.018
	$^4F^o_{9/2}$	517082	517171	0.017
	$^4P^o_{5/2}$	548038	548037	−0.000
	$^4D^o_{3/2}$	549745	549713	−0.006
	$^4D^o_{1/2}$	551073	550994	−0.014
	$^4P^o_{1/2}$	554732	554864	0.024
	$^4P^o_{3/2}$	555373	555472	0.018
	$^4D^o_{7/2}$	555589	555583	−0.001
	$^4D^o_{5/2}$	555748	555759	0.002
	$^4D^o_{3/2}$	567493	567465	−0.005
	$^4D^o_{5/2}$	567645	567610	−0.006
	$^4F^o_{5/2}$	592986	592959	−0.005
	$^4P^o_{7/2}$	600681	600643	−0.006
	$^4P^o_{3/2}$	644322	643917	−0.063
	$^4P^o_{1/2}$	647995	647577	−0.065
$3s3p[^1P]3d$	$^4F^o_{7/2}$	650132	649771	−0.056
	$^4F^o_{5/2}$	651881	651550	−0.051
	$^4P^o_{1/2}$	668547	668411	−0.020
	$^4D^o_{3/2}$	669536	669304	−0.035
	$^4P^o_{3/2}$	672173	671902	−0.040
	$^4D^o_{5/2}$	673362	672939	−0.063

decay channels only). We discuss the levels in this sequence, before showing how they are connected in plasma diagnostics and in some lifetime measurements. For an example (Fe XIV) of our results on transition rates and level lifetimes, see table 15.

4.1. $3s^23p\,^2P^o_{3/2}$ level

The magnetic dipole (M1) transitions between the fine structure levels of the ground configuration of B-, F-, Al- and Cl-like ions figure prominently in the observations and interpretation of solar and stellar coronae and of low-density laboratory plasmas. They represent radiative decay after excitation to the lowest excited levels of these ions and thus serve as tracers that indicate the presence of a given element and charge state and therefore help to estimate the plasma temperature. However, in a low-density plasma the collision rate for such excitation is often comparable to the M1 radiative decay rate; hence, the upper level population depends on the collision rate and thus on density. Depending on the population balance of the lowest levels, certain line intensity ratios in the spectra can then be used as a plasma diagnostic tool that reveals the density. Since there are many pathways to excitation and deexcitation, collisional-radiative models are employed to take into account hundreds or thousands of levels and tens of thousands of transitions. Very few experimental data exist or will ever become available for the transition rates especially between high-lying levels. Most transitions between low- and high-lying levels can be approximated by using hydrogenic wave functions. In practice, of ions

Table 6. Comparison of second-order MR-MP calculated energies (in cm^{-1}) and NIST experimental values in Cr^{11+}.

Configuration	Level	MR-MP	NIST	Deviation (per cent)
$3s^23p$	$^2P^o_{1/2}$	0	0	0
	$^2P^o_{3/2}$	12262	12261	−0.008
$3s3p^2$	$^4P_{1/2}$	192096	192120	0.012
	$^4P_{3/2}$	196900	196911	0.006
	$^4P_{5/2}$	203332	203349	0.008
	$^2D_{3/2}$	254402	254428	0.010
	$^2D_{5/2}$	255537	255566	0.011
	$^2S_{1/2}$	313809	313745	−0.020
	$^2P_{1/2}$	333197	333196	−0.000
	$^2P_{3/2}$	339257	339251	−0.002
$3s^23d$	$^2D_{3/2}$	408659	408640	−0.005
	$^2D_{5/2}$	409776	409741	−0.009
$3p^3$	$^2D^o_{3/2}$	493361	493437	0.015
	$^2D^o_{5/2}$	495309	495368	0.012
	$^4S^o_{3/2}$	504345	504431	0.017
	$^2P^o_{1/2}$	550161	550208	0.009
	$^2P^o_{3/2}$	551751	551641	−0.020
$3s3p[^3P]3d$	$^4F^o_{3/2}$	552098		
	$^4F^o_{5/2}$	554738	554899	0.029
	$^4F^o_{7/2}$	558535	558684	0.027
	$^4F^o_{9/2}$	563750	563915	0.029
	$^4P^o_{5/2}$	594933	594946	0.002
	$^4D^o_{3/2}$	596839	596837	−0.000
	$^4D^o_{1/2}$	598195	598172	−0.004
	$^4P^o_{1/2}$	603492	603600	0.018
	$^4D^o_{7/2}$	603967	603995	0.005
	$^4P^o_{3/2}$	604035	604158	0.020
	$^4D^o_{5/2}$	604304	604331	0.004
	$^4D^o_{3/2}$	616538	616498	−0.006
	$^4D^o_{5/2}$	616805	616790	−0.002
	$^4F^o_{5/2}$	643104	643089	−0.002
	$^4P^o_{7/2}$	652825	652796	−0.004
	$^4P^o_{3/2}$	698116	697756	−0.052
	$^4P^o_{1/2}$	702965		
$3s3p[^1P]3d$	$^4F^o_{7/2}$	705269	704993	−0.039
	$^4F^o_{5/2}$	707396	707142	0.036
	$^4P^o_{1/2}$	724795	724656	0.019
	$^4D^o_{3/2}$	726053	725710	0.047
	$^4P^o_{3/2}$	728341	728200	0.019
	$^4D^o_{5/2}$	729650	729281	0.051

Table 7. Comparison of second-order MR-MP calculated energies (in cm^{-1}) and NIST experimental values in Mn^{12+}.

Configuration	Level	MR-MP	NIST	Deviation (per cent)
$3s^23p$	$^2P^o_{1/2}$	0	0	0
	$^2P^o_{3/2}$	15296	15295	−0.007
$3s3p^2$	$^4P_{1/2}$	208409	208451	0.020
	$^4P_{3/2}$	214524	214546	0.010
	$^4P_{5/2}$	222434	222463	0.013
	$^2D_{3/2}$	276474	276497	0.008
	$^2D_{5/2}$	278072	278099	0.010
	$^2S_{1/2}$	339052	339001	−0.015
	$^2P_{1/2}$	360388	360387	−0.000
	$^2P_{3/2}$	367435	367425	−0.003
$3s^23d$	$^2D_{3/2}$	440719	440725	0.001
	$^2D_{5/2}$	442231	442220	0.002
$3p^3$	$^2D^o_{3/2}$	534469	534492	0.004
	$^2D^o_{5/2}$	537209	537263	0.010
	$^4S^o_{3/2}$	546074	546178	0.019
	$^2P^o_{1/2}$	595629	595637	0.001
	$^2P^o_{3/2}$	598030	597797	−0.039
$3s3p[^3P]3d$	$^4F^o_{3/2}$	596675		
	$^4F^o_{5/2}$	599975		
	$^4F^o_{7/2}$	604753		
	$^4F^o_{9/2}$	611382	611495	0.018
	$^4P^o_{5/2}$	642308	642337	0.005
	$^4D^o_{3/2}$	644434	644449	0.002
	$^4D^o_{1/2}$	645847	645856	0.001
	$^4P^o_{1/2}$	653099	653189	0.014
	$^4D^o_{7/2}$	653163	653217	0.008
	$^4P^o_{3/2}$	653564	653697	0.020
	$^4D^o_{5/2}$	653698	653739	0.006
	$^4D^o_{3/2}$	666406	666369	0.006
	$^4D^o_{5/2}$	666826	666826	0.000
	$^4F^o_{5/2}$	693721	693715	0.001
	$^4P^o_{7/2}$	705826	705799	0.004
	$^4P^o_{3/2}$	752439	752115	0.043
	$^4P^o_{1/2}$	758731		
$3s3p[^1P]3d$	$^4F^o_{7/2}$	761090	760881	−0.027
	$^4F^o_{5/2}$	763631	763441	0.025
	$^4P^o_{1/2}$	781730	781703	0.003
	$^4D^o_{3/2}$	783168	782845	0.041
	$^4P^o_{3/2}$	785474	785391	0.011
	$^4D^o_{5/2}$	786733	786405	0.042

of iron group elements, only some in-shell transition rates have been measured by beam-foil spectroscopy, and some of the E1-forbidden transition rates have been determined experimentally by employing either a heavy-ion storage ring or an EBIT. It is exactly the latter transition rates that matter most as a testable parameter in the collisional-radiative models. Consequently, these M1 rates (the small E2 admixture amounts to less than 0.1% in the Al-like ions of interest) have been calculated frequently (see [67]), but with varying success (see figure 1).

At a first glance, most of the results (for the example of Fe XIV) fall into a very narrow interval, while very few deviate drastically from that majority. A closer inspection, however, reveals that most of the theoretical results are actually not the results of extensive calculations, but of the so-called 'semiempirical adjustments' to the extensively calculated values. This seemed appropriate, because in a straightforward approximation (near the nonrelativistic limit and assuming rather pure configurations), the M1 transition rate between fine structure levels of a given term is the product of the line strength S and the third power of the transition energy ΔE. For the transition of interest in the ground term of Al-like ions, Racah algebra in this approximation yields $S = \frac{4}{3}$, and the transition energy is available with high accuracy from spectroscopic observations. If a calculation does not determine the transition energy correctly, it is quite customary to replace the faulty energy difference by the experimental data—the aforementioned 'semiempirical'

Table 8. Comparison of second-order MR-MP calculated energies (in cm^{-1}) and NIST experimental values in Fe^{13+}.

Configuration	Level	MR-MP	NIST	Deviation (per cent)
$3s^23p$	$^2P^o_{1/2}$	0	0	0
	$^2P^o_{3/2}$	18852	18852.5	0.003
$3s3p^2$	$^4P_{1/2}$	225090	225114	0.011
	$^4P_{3/2}$	232794	232789	−0.002
	$^4P_{5/2}$	242386	242387	0.000
	$^2D_{3/2}$	299231	299242	0.004
	$^2D_{5/2}$	301452	301469	0.006
	$^2S_{1/2}$	364717	364693	−0.007
	$^2P_{1/2}$	388502	388510	0.002
	$^2P_{3/2}$	396516	396512	−0.001
$3s^23d$	$^2D_{3/2}$	473188	473223	0.007
	$^2D_{5/2}$	475185	475202	0.001
$3p^3$	$^2D^o_{3/2}$	576407	576388	−0.004
	$^2D^o_{5/2}$	580226	580233	0.001
	$^4S^o_{3/2}$	588916	589002	0.015
	$^2P^o_{1/2}$	642236	642310	0.012
	$^2P^o_{3/2}$	645732	645409	−0.050
$3s3p[^3P]3d$	$^4F^o_{3/2}$	641822		
	$^4F^o_{5/2}$	645891	645988	0.015
	$^4F^o_{7/2}$	651824	651946	0.019
	$^4F^o_{9/2}$	660153	660263	0.017
	$^4P^o_{5/2}$	690300	690304	0.001
	$^4D^o_{3/2}$	692673	692662	−0.002
	$^4D^o_{1/2}$	694166	694166	0.000
	$^4D^o_{7/2}$	703359	703393	0.005
	$^4P^o_{1/2}$	703723	703750	0.004
	$^4D^o_{5/2}$	704095	704114	0.003
	$^4P^o_{3/2}$	704123	704209	0.012
	$^4D^o_{3/2}$	717245	717195	−0.007
	$^4D^o_{5/2}$	717863	717861	−0.000
	$^4F^o_{5/2}$	744955	744965	0.001
	$^4P^o_{7/2}$	759833	759814	−0.003
	$^4P^o_{3/2}$	807380	807113	−0.033
	$^4P^o_{1/2}$	815419	815123	−0.036
$3s3p[^1P]3d$	$^4F^o_{7/2}$	817734	817593	0.017
	$^4F^o_{5/2}$	820724	820601	−0.015
	$^4P^o_{1/2}$	839475	839492	0.002
	$^4D^o_{3/2}$	841040	840775	−0.032
	$^4P^o_{3/2}$	843700	843656	−0.005
	$^4D^o_{5/2}$	844757	844477	−0.033

Table 9. Comparison of second-order MR-MP calculated energies (in cm^{-1}) and NIST experimental values in Co^{14+}.

Configuration	Level	MR-MP	NIST	Deviation (per cent)
$3s^23p$	$^2P^o_{1/2}$	0	0	0
	$^2P^o_{3/2}$	22987	22979	−0.035
$3s3p^2$	$^4P_{1/2}$	242094	242124	0.012
	$^4P_{3/2}$	251709	251699	−0.004
	$^4P_{5/2}$	263194	263189	−0.002
	$^2D_{3/2}$	322723	322725	0.001
	$^2D_{5/2}$	325772	325790	0.006
	$^2S_{1/2}$	390874	390855	−0.005
	$^2P_{1/2}$	417713	417717	0.001
	$^2P_{3/2}$	426634	426629	−0.001
$3s^23d$	$^2D_{3/2}$	506176	506230	0.011
	$^2D_{5/2}$	508756	508793	0.007
$3p^3$	$^2D^o_{3/2}$	619153	619050	−0.017
	$^2D^o_{5/2}$	624416	624445	0.005
	$^4S^o_{3/2}$	632936	633036	0.016
	$^2P^o_{1/2}$	690102	690171	0.010
	$^2P^o_{3/2}$	695034	694620	−0.060
$3s3p[^3P]3d$	$^4F^o_{5/2}$	692512	692464	−0.007
	$^4F^o_{3/2}$	687552		
	$^4F^o_{7/2}$	699794	699778	−0.002
	$^4F^o_{9/2}$	710151	710230	0.011
	$^4P^o_{5/2}$	738948	738955	0.001
	$^4D^o_{3/2}$	741601	741602	0.000
	$^4D^o_{1/2}$	743187	743224	0.005
	$^4D^o_{7/2}$	754639	754674	0.005
	$^4P^o_{1/2}$	755443		
	$^4D^o_{5/2}$	755568	755594	0.003
	$^4P^o_{3/2}$	755783		
	$^4D^o_{3/2}$	769173	769138	−0.005
	$^4D^o_{5/2}$	770032	770046	0.002
	$^4F^o_{5/2}$	796959	796989	0.004
	$^4P^o_{7/2}$	815026	815014	−0.001
	$^4P^o_{3/2}$	863127	862878	−0.029
	$^4P^o_{1/2}$	873267		
$3s3p[^1P]3d$	$^4F^o_{7/2}$	875384	875288	−0.011
	$^4F^o_{5/2}$	878849	878778	0.008
	$^4P^o_{1/2}$	898217	898240	0.003
	$^4D^o_{3/2}$	899955	899693	0.029
	$^4P^o_{3/2}$	903160	903152	−0.001
	$^4D^o_{5/2}$	903931	903677	−0.028

correction. Most calculations did not achieve good agreement with the experimental transition energy (the fine structure interval), but after the correction one does not see that shortfall of an extensive calculational effort. So the few deviant theory results displayed in figure 1 are those that were not corrected and thus give a more honest presentation of the shortcomings of earlier calculations. There also are early *ab initio* calculations that—although working with rather few wave functions—come close to the expected result, but only in this particular case (and not in others); here the agreement has to be considered as merely incidental.

We note that our own computational technique has determined the ground state fine structure interval in Fe XIV very close to the experimental value, so that no semiempirical correction was necessary [52]. The calculated $3s^23p\,^2P^o_{3/2}$ level lifetime agrees with the result of a measurement at the Livermore EBIT [68]. The calculation did not comprise a QED correction to the M1 transition operator that has since been discussed [69, 70]. This QED correction increases the transition rate by a factor $(1+2\alpha/\pi)$, or by 0.45%. After this correction, the MR-MP result slightly disagrees with the Livermore result. (Agreement within one standard deviation of the experimental result would be restored, if the experiment suffered from a systematic error discussed below and was corrected accordingly.) The Heidelberg EBIT group has measured the same atomic system and has claimed an error bar of only 0.1%. At this level of precision, the experimental finding disagrees with all calculations. We will

Table 10. Comparison of second-order MR-MP calculated energies (in cm^{-1}) and NIST experimental values in Ni^{15+}.

Configuration	Level	MR-MP	NIST	Deviation (per cent)
$3s^23p$	$^2P^o_{1/2}$	0	0	0
	$^2P^o_{3/2}$	27759	27760.4	0.005
$3s3p^2$	$^4P_{1/2}$	259466	259489	0.009
	$^4P_{3/2}$	271367	271341	−0.010
	$^4P_{5/2}$	284954	284949	−0.002
	$^2D_{3/2}$	347030	347032	0.001
	$^2D_{5/2}$	351166	351185	0.005
	$^2S_{1/2}$	417542	417523	−0.005
	$^2P_{1/2}$	448160	448169	0.002
	$^2P_{3/2}$	457900	457912	0.003
$3s^23d$	$^2D_{3/2}$	539769	539839	0.013
	$^2D_{5/2}$	543041	543107	0.012
$3p^3$	$^2D^o_{3/2}$	662774	662678	0.014
	$^2D^o_{5/2}$	669939	669946	0.001
	$^4S^o_{3/2}$	678316	678418	0.015
	$^2P^o_{1/2}$	739369	739500	0.018
	$^2P^o_{3/2}$	746137	746100	−0.005
$3s3p[^3P]3d$	$^4F^o_{3/2}$	733983		
	$^4F^o_{5/2}$	739964		
	$^4F^o_{7/2}$	748806		
	$^4F^o_{9/2}$	761568	761641	−0.010
	$^4P^o_{5/2}$	788390	788399	0.001
	$^4D^o_{3/2}$	791357	791390	0.004
	$^4D^o_{1/2}$	793043	793115	0.009
	$^4D^o_{7/2}$	807192	807214	0.003
	$^4D^o_{5/2}$	808291	808316	0.003
	$^4P^o_{1/2}$	808438		
	$^4P^o_{3/2}$	808721		
	$^4D^o_{3/2}$	822351	822364	0.002
	$^4D^o_{5/2}$	823484	823538	0.007
	$^4F^o_{5/2}$	849869	849946	0.009
	$^4P^o_{7/2}$	871561	871583	0.003
	$^4P^o_{3/2}$	919765	919543	−0.024
	$^4P^o_{1/2}$	932400		
$3s3p[^1P]3d$	$^4F^o_{7/2}$	934186	934137	0.005
	$^4F^o_{5/2}$	938146	938122	−0.003
	$^4P^o_{1/2}$	958094	958134	0.004
	$^4D^o_{3/2}$	960119		
	$^4P^o_{3/2}$	963960	963961	0.000
	$^4D^o_{5/2}$	964409		

Table 11. Comparison of second-order MR-MP calculated energies (in cm^{-1}) and NIST experimental values in Cu^{16+}.

Configuration	Level	MR-MP	NIST	Deviation (per cent)
$3s^23p$	$^2P^o_{1/2}$	0	0	0
	$^2P^o_{3/2}$	33235	33239	0.012
$3s3p^2$	$^4P_{1/2}$	277216	277231	0.005
	$^4P_{3/2}$	291837	291810	0.009
	$^4P_{5/2}$	307733	307708	0.008
	$^2D_{3/2}$	372227	372236	0.002
	$^2D_{5/2}$	377770	377783	0.003
	$^2S_{1/2}$	444775	444759	0.004
	$^2P_{1/2}$	479992	480016	0.005
	$^2P_{3/2}$	490438	490467	0.006
$3s^23d$	$^2D_{3/2}$	574060	574180	0.021
	$^2D_{5/2}$	578141	578243	0.018
$3p^3$	$^2D^o_{3/2}$	707310		
	$^2D^o_{5/2}$	716925		
	$^4S^o_{3/2}$	725208	725320	0.015
	$^2P^o_{1/2}$	790181		
	$^2P^o_{3/2}$	799245		
$3s3p[^3P]3d$	$^4F^o_{3/2}$	781201		
	$^4F^o_{5/2}$	788341		
	$^4F^o_{7/2}$	798971		
	$^4F^o_{9/2}$	814569		
	$^4P^o_{5/2}$	838734		
	$^4D^o_{3/2}$	842050		
	$^4D^o_{1/2}$	843832		
	$^4D^o_{7/2}$	861178	861003	−0.020
	$^4D^o_{5/2}$	862412	856728	−0.663
	$^4P^o_{1/2}$	862861		
	$^4P^o_{3/2}$	863087		
	$^4D^o_{3/2}$	876925		
	$^4D^o_{5/2}$	878344	876785	−0.178
	$^4F^o_{5/2}$	903850	909161	0.584
	$^4P^o_{7/2}$	929605	931186	0.170
	$^4P^o_{3/2}$	977417		
	$^4P^o_{1/2}$	992982		
$3s3p[^1P]3d$	$^4F^o_{7/2}$	994301		
	$^4F^o_{5/2}$	998764		
	$^4P^o_{1/2}$	1019261		
	$^4D^o_{3/2}$	1021739		
	$^4P^o_{3/2}$	1026248		
	$^4D^o_{5/2}$	1026365		

discuss this problem in the context of experiments below. In table 16, we list our calculated level lifetimes for the range of Al-like ions from K through Ge.

4.2. $3s3p^2\,{}^4P_J$ levels

The (spin-changing) intercombination decay rate of the lowest quartet levels is much higher than the M1 transition rate discussed above. The order of magnitude of the level lifetimes (for Fe XIV) is 100 ns versus 17 ms. The many-nanosecond lifetime range is accessible by beam-foil spectroscopy, and the intercombination transitions in Al-like ions of Fe, Co, Ni, Cu and Zn (see [24, 25] and later papers by the same authors) were detected by beam-foil spectroscopy at Bochum at around the same time as Sugar *et al* reported the lines for ions of Cu through Mo from a tokamak [26]. The beam-foil observations were not very accurate, but they made it possible to recognize the same lines in EUV spectra of the solar corona, where the wavelengths had been measured with much better accuracy, but where the lines had remained unidentified. The Bochum beam-foil work was extended to Br at Argonne [41] and to Au at GSI Darmstadt [44, 45], including some lifetime determinations. A group from Lund pursued similar work at RIKEN (Japan), but their lifetime results follow a different isoelectronic trend that disagrees with theory [42, 43]. At the low-Z end of the isoelectronic sequence, Si^+ has been studied in a radiofrequency ion trap [71]. For moderate charge states, the isoelectronic trends of the fine structure intervals of the quartet levels have been systematized on the basis of the experimental data [25, 46]. Such data of sufficient quality

Table 12. Comparison of second-order MR-MP calculated energies (in cm^{-1}) and NIST experimental values in Zn^{17+}.

Configuration	Level	MR-MP	NIST	Deviation (per cent)
$3s^23p$	$^2P^o_{1/2}$	0	0	0
	$^2P^o_{3/2}$	39479	39483	0.010
$3s3p^2$	$^4P_{1/2}$	295343	295200	−0.048
	$^4P_{3/2}$	313181	312993	0.060
	$^4P_{5/2}$	331582	331359	−0.067
	$^2D_{3/2}$	398381	398390	0.002
	$^2D_{5/2}$	405728	405760	0.008
	$^2S_{1/2}$	472635	472601	−0.007
	$^2P_{1/2}$	513359	513373	0.003
	$^2P_{3/2}$	524378	524382	0.001
$3s^23d$	$^2D_{3/2}$	609150	609252	0.017
	$^2D_{5/2}$	614166	614272	0.017
$3p^3$	$^2D^o_{3/2}$	752796		
	$^2D^o_{5/2}$	765496		
	$^4S^o_{3/2}$	773750	773682	−0.009
	$^2P^o_{1/2}$	842676		
	$^2P^o_{3/2}$	854547		
$3s3p[^3P]3d$	$^4F^o_{3/2}$	829286		
	$^4F^o_{5/2}$	837734		
	$^4F^o_{7/2}$	850395		
	$^4F^o_{9/2}$	869318		
	$^4P^o_{5/2}$	890082		
	$^4D^o_{3/2}$	893782		
	$^4D^o_{1/2}$	895643		
	$^4D^o_{7/2}$	916758		
	$^4D^o_{5/2}$	918075		
	$^4P^o_{1/2}$	918860		
	$^4P^o_{3/2}$	919028		
	$^4D^o_{3/2}$	933041		
	$^4D^o_{5/2}$	934708		
	$^4F^o_{5/2}$	959094		
	$^4P^o_{7/2}$	989327		
	$^4P^o_{3/2}$	1036210		
	$^4P^o_{1/2}$	1055173		
$3s3p[^1P]3d$	$^4F^o_{7/2}$	1055896		
	$^4F^o_{5/2}$	1060860		
	$^4P^o_{1/2}$	1081888		
	$^4D^o_{3/2}$	1085020		
	$^4D^o_{5/2}$	1089979		
	$^4P^o_{3/2}$	1090194		

Table 13. Comparison of second-order MR-MP calculated energies (in cm^{-1}) and NIST experimental values in Ga^{18+}.

Configuration	Level	MR-MP	NIST	Deviation (per cent)
$3s^23p$	$^2P^o_{1/2}$	0	0	0
	$^2P^o_{3/2}$	46564	46584	0.043
$3s3p^2$	$^4P_{1/2}$	313855		
	$^4P_{3/2}$	335482		
	$^4P_{5/2}$	356566		
	$^2D_{3/2}$	425572	425568	−0.001
	$^2D_{5/2}$	435204	435260	0.013
	$^2S_{1/2}$	501201	501163	−0.008
	$^2P_{1/2}$	548416	548398	−0.003
	$^2P_{3/2}$	559855	559837	−0.003
$3s^23d$	$^2D_{3/2}$	645141	645235	0.015
	$^2D_{5/2}$	651220	651354	0.021
$3p^3$	$^2D^o_{3/2}$	799298		
	$^2D^o_{5/2}$	815793		
	$^4S^o_{3/2}$	824097		
	$^2P^o_{1/2}$	897017		
	$^2P^o_{3/2}$	912241		
$3s3p[^3P]3d$	$^4F^o_{3/2}$	878333		
	$^4F^o_{5/2}$	888243		
	$^4F^o_{7/2}$	903190		
	$^4F^o_{9/2}$	925995		
	$^4P^o_{5/2}$	942546		
	$^4D^o_{3/2}$	946678		
	$^4D^o_{1/2}$	948576		
	$^4D^o_{7/2}$	974103		
	$^4D^o_{5/2}$	975440		
	$^4P^o_{1/2}$	976601		
	$^4P^o_{3/2}$	976708		
	$^4D^o_{3/2}$	990850		
	$^4D^o_{5/2}$	992636		
	$^4F^o_{5/2}$	1015851		
	$^4P^o_{7/2}$	1050903		
	$^4P^o_{3/2}$	1096284		
	$^4P^o_{1/2}$	1119143		
$3s3p[^1P]3d$	$^4F^o_{7/2}$	1119148		
	$^4F^o_{5/2}$	1124592		
	$^4P^o_{1/2}$	1146149		
	$^4D^o_{3/2}$	1150163		
	$^4D^o_{5/2}$	1155438		
	$^4P^o_{3/2}$	1155981		

are not yet available for most low-charge state ions of the Al isoelectronic sequence, because in most plasmas the emission of the ions in long-lived low quartet levels would be quenched by collisions.

4.3. 3s3p3d $^4F^o_{9/2}$ level

The 3s3p3d $^4F^o_{9/2}$ level might seem to be of little interest, because it has a J value so high that there is no dipole or quadrupole excitation from the ground term, and the 3s3p3d configuration is multiply excited. It is probably for these reasons that various calculations of energy levels have left out this level altogether, even when explicitly treating the other levels of the same quartet term. The level values of some of the 3s3p3d $^4F^o_J$ levels in Al-like ions of iron group elements have first be determined by Churilov and Levashov [49] who obtained these data as the lower levels of decays that started out from $3p^23d$ and $3s3d^2$ levels in a laser-produced plasma. Practically coincidentally, but employing a very different technique, several of the levels were seen in emission after foil excitation of fast ion beams [48]. The latter experiment exploited the relative longevity of the high angular momentum quartet levels ($J = \frac{3}{2}$ to $\frac{7}{2}$) with their lifetimes in the nanosecond range (whereas most other levels and thus spectral lines featured picosecond lifetimes). Waiting (in the experiment, after excitation has ended) until the short-lived levels have decayed, the delayed spectrum is expected to be relatively enriched in contributions from long-lived levels, but, of course, over time all of the decay curves are being reduced in intensity. Owing to a low

Table 14. Comparison of second-order MR-MP calculated energies (in cm^{-1}) and NIST experimental values in Ge^{19+}.

Configuration	Level	MR-MP	NIST	Deviation (per cent)
$3s^23p$	$^2P^o_{1/2}$	0	0	0
	$^2P^o_{3/2}$	54562	54564	0.004
$3s3p^2$	$^4P_{1/2}$	332749		
	$^4P_{3/2}$	358815		
	$^4P_{5/2}$	382743		
	$^2D_{3/2}$	453877	453869	−0.002
	$^2D_{5/2}$	466367	466407	0.009
	$^2S_{1/2}$	530558	530521	−0.007
	$^2P_{1/2}$	585318	585257	0.010
	$^2P_{3/2}$	597008	597020	0.002
$3s^23d$	$^2D_{3/2}$	682141	682246	0.015
	$^2D_{5/2}$	689414	689533	0.017
$3p^3$	$^2D^o_{3/2}$	846885		
	$^2D^o_{5/2}$	867950		
	$^4S^o_{3/2}$	876391	875850	0.062
	$^2P^o_{1/2}$	953363		
	$^2P^o_{3/2}$	972492		
$3s3p[^3P]3d$	$^4F^o_{3/2}$	928436		
	$^4F^o_{5/2}$	939968		
	$^4F^o_{7/2}$	957466	1000790	4.52
	$^4F^o_{9/2}$	984782	1002640	1.81
	$^4P^o_{5/2}$	996239	996200	−0.004
	$^4D^o_{3/2}$	1000881		
	$^4D^o_{1/2}$	1002722		
	$^4D^o_{7/2}$	1033390	1033390	0.000
	$^4D^o_{5/2}$	1034665		
	$^4P^o_{1/2}$	1036246	1035630	−0.059
	$^4P^o_{3/2}$	1036292		
	$^4D^o_{3/2}$	1050501	1050590	0.008
	$^4D^o_{5/2}$	1052112		
	$^4F^o_{5/2}$	1074450		
	$^4P^o_{7/2}$	1114514	1114490	−0.002
	$^4P^o_{3/2}$	1157787	1157630	−0.014
$3s3p[^1P]3d$	$^4F^o_{7/2}$	1184236	1184750	0.043
	$^4P^o_{1/2}$	1185058	1184190	−0.073
	$^4F^o_{5/2}$	1190124	1190040	−0.007
	$^4P^o_{1/2}$	1212228	1211960	−0.022
	$^4D^o_{3/2}$	1217365	1217450	0.007
	$^4D^o_{5/2}$	1222930	1222780	−0.012
	$^4P^o_{3/2}$	1223805	1223700	−0.009

Table 15. Calculated E1/M1/E2/M2 transition probabilities A and lifetimes τ of $3s^23p\,^2P^o_{3/2}$, $3s3p^2\,^4P_J$ and $3s3p3d\,^4F^o_{9/2}$ levels in aluminium-like Fe^{13+}. $a(b)$ means $a \times 10^b$.

Upper(j) → Lower (i)	ΔE (cm^{-1})	A_{ji}(s^{-1})	τ (μs)
Fe^{+13}			
$^2P^o_{3/2} \to {}^2P^o_{1/2}$	18852	M1: 6.016(+1)	
		E2: 1.466(−2)[a]	16620
		1.484(−2)[b]	
$^4F^o_{9/2} \to {}^4F^o_{7/2}$	8329	M1: 1.541(+1)	
		E2: 1.628(−4)[a]	
		1.724(−4)[b]	
$\to {}^4F^o_{5/2}$	14262	E2: 2.096(−4)[a]	
		2.228(−4)[b]	
$\to {}^2D^o_{5/2}$	79927	E2: 2.691(−3)[a]	
		2.875(−3)[b]	
$\to {}^2D_{5/2}$	184968	M2: 2.423(−1)	
$\to {}^2D_{5/2}$	358701	M2: 3.375(+1)	
$\to {}^4P_{5/2}$	417767	M2: 3.361(+0)	18950
$^4P_{5/2} \to {}^4P_{3/2}$	9592	M1: 1.411(+1)	
		E2: 4.976(−4)[a]	
		5.097(−4)[b]	
$\to {}^4P_{1/2}$	17296	E2: 3.274(−3)[a]	
		7.160(−3)[b]	
$\to {}^2P^o_{3/2}$	223534	E1: 2.256(+7)[a]	
		2.064(+7)[b]	
		M2: 1.685(+0)	
$\to {}^2P^o_{1/2}$	242386	M2: 1.423(+0)	0.04433
$^4P_{3/2} \to {}^4P_{1/2}$	7704	M1: 1.014(+1)	
		E2: 1.003(−5)[a]	
		2.099(−5)[b]	
$\to {}^2P^o_{3/2}$	213942	E1: 5.458(+6)[a]	
		4.851(+6)[b]	
		M2: 6.838(−2)	
$\to {}^2P^o_{1/2}$	232794	E1: 4.833(+5)[a]	
		4.640(+5)[b]	
		M2: 2.193(+0)	0.1683
$^4P_{1/2} \to {}^4P^o_{3/2}$	206238	M2: 2.892(−1)	
		E1: 8.693(+6)[a]	
		7.885(+6)[b]	
$\to {}^2P^o_{1/2}$	225090	E1: 2.230(+7)[a]	0.0323

[a]In Babushkin gauge. [b]In Coulomb gauge.

signal rate, the spectral resolution had to be no better than moderate, and some spectral blends were unavoidable. Hence, while the lifetime pattern reported is qualitatively compatible with various calculations, the experimental lifetime data are not good enough for a meaningful comparison with theory in quantitative detail. The beam-foil technique was not suitable to deal with the much longer lifetime of the $3s3p3d\,^4F^o_{9/2}$ level for which calculations apparently did not even exist at the time. Later calculations pointed to the millisecond range, that is, to a lifetime six orders of magnitude longer than those of the three other fine structure levels of the same term. (A similarly wide range of fine structure level lifetimes is found for the $3s^23p3d\ ^3F^o$ term in Si-like ions, where $J = 4$ is the long-lived fine structure level [72, 85].) The calculated lifetimes of the $3s3p3d\,^4F^o_{9/2}$ level in the ions of present interest are included in table 16.

4.4. Cascade problem in measurements

In the middle of the iron group of elements, the lifetimes of the $3s^23p\ ^2P^o_{3/2}$ level and the $3s3p3d\,^4F^o_{9/2}$ level turn out to be rather similar to each other (see figure 2). This may be seen as a curiosity of little consequence. However, in a recent lifetime measurement of a heavy-ion storage ring, the similarity has caused a sizeable systematic error [72]. On its own, this finding would also be of rather limited interest, but it might pertain—to a much smaller extent, but of a relatively high importance—to the extremely precise lifetime measurements performed at the Heidelberg EBIT [69, 70]. The details of the causal chain are yet to be determined, but preliminary radiative-collisional modeling estimates indicate

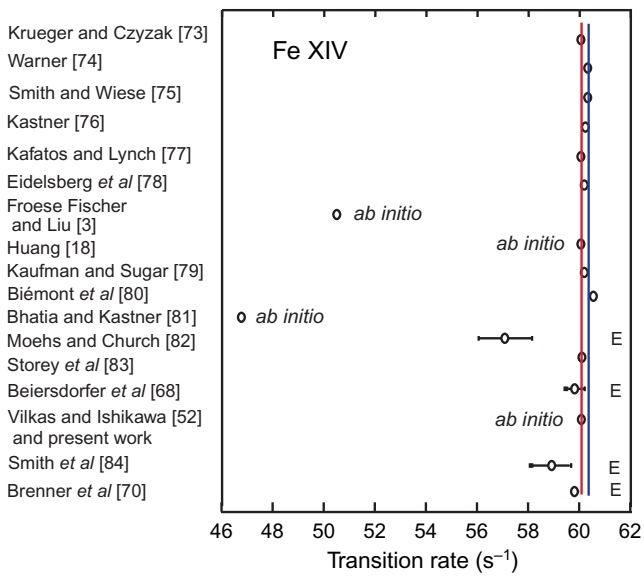

Figure 1. Historic timeline of the calculated and measured (E) M1 transition rate in the ground state of Fe XIV. The vertical red (left) line indicates the expected value based on the experimental term difference and a line strength $S = \frac{4}{3}$; the vertical blue (right) line represents the same after the application of the QED correction to the M1 transition operator. The present lifetime result is similar to the entry for Vilkas and Ishikawa [52], which has been obtained by the same technique as was used in the present work. Many of the other entries are mostly of historic interest by now: Krueger and Czyzak [73]; Warner [74]; Smith and Wiese [75]; Kastner [76]; Kafatos and Lynch [77]; Eidelsberg *et al* [78]; Froese Fischer and Liu [3]; Huang [18]; Kaufman and Sugar [79]; Biémont *et al* [80]; Bhatia and Kastner [81]; Moehs and Church [82]; Storey *et al* [83]; Beiersdorfer *et al* [68]; Vilkas and Ishikawa [52]; Smith *et al* [84]; Brenner *et al* [70]. For earlier presentations and reviews of the data on Al-like ion M1 lifetimes, and more of the experimental context, see [68, 70, 85, 86].

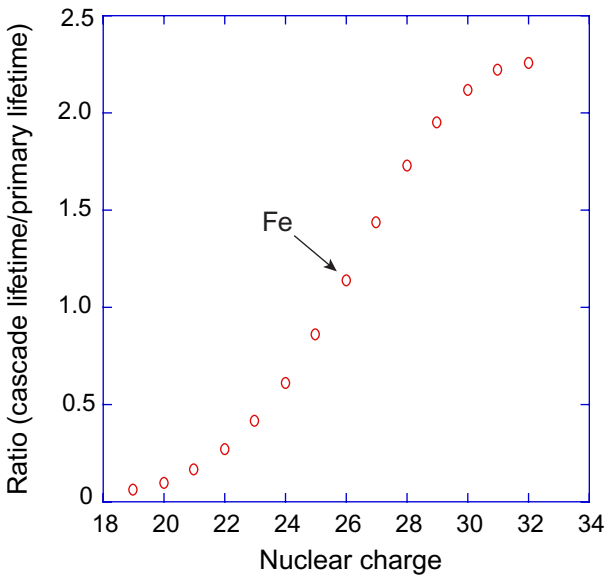

Figure 2. Ratio of lifetimes of the $3s3p3d\,^4F^o_{9/2}$ (cascade) and the $3s^23p\,^2P^o_{3/2}$ (primary decay) levels.

that the cascade from the $3s3p3d\,^4F^o_{9/2}$ level might cause a shift of the apparent $3s^23p\,^2P^o_{3/2}$ level lifetime by a small fraction of 1%, and thus by clearly more than the present error estimate of that experiment—an experiment the lifetime result of which disagrees with modern quantum mechanical calculations that take all known QED contributions (to the energy and to the M1 transition operator) into account. In Fe XIV, our MR-MP calculations indicate three major decay branches of the $3s3p3d\,^4F^o_{9/2}$ level: an M1 transition with a branch fraction of 29.3% leads to the $3s3p3d\,^4F^o_{7/2}$ level from which in turn E1 transitions feed the $3s^23d\,^2D$ and $3s3p^2\,^2D$ and ^4P $J = \frac{5}{2}$ levels, all of which feed into $3s^23p\,^2P^o_{3/2}$. From the same original level, M2 transitions with branch fractions of 64.3 and 6.4%, respectively, lead directly to the same $3s^23d\,^2D$, $3s3p^2\,^2D$ and $3s3p^2\,^4P$ $J = \frac{5}{2}$ levels. Practically the complete population of the $3s3p3d\,^4F^o_{9/2}$ level thus feeds the $3s^23p\,^2P^o_{3/2}$ level, the upper one of the fine structure levels of the ground term. When recording and analyzing decay curves of the $^2P^o_{3/2}$ level in Fe XIV, the lifetimes of the primary decay and the specific cascade cannot be separated by multi-exponential analysis. However, because of the Z^4 scaling of fine structure splittings, the M1 decay rate in the $3s3p3d\,^4F^o$ term grows faster with nuclear charge Z than the M2 decay rates, giving the M1 decay a branch fraction of almost 50% in Ni XVI, while the overall cascade picture remains the same. The lifetime difference, nevertheless, becomes large enough to actually see the two different lifetime components in the decay curve, with fit results that corroborate the present calculations [72].

5. Discussion and conclusions

The present study demonstrates how a large body of experimental data on atomic levels can be checked for consistency against the results of *ab initio* calculations that reach close to spectroscopic accuracy without parametrizations or semiempirical adjustments. In this way it becomes apparent where experimental problems remain to be overcome. The question arises, of course, whether it would be cost effective to close the gaps in the database by further experiments or—given the present high level of accuracy of our calculations—by computation, once the quality of the method has been ascertained. Certainly calculations need to be checked against good experimental data, and, similarly, dedicated experiments may be more accurate than any approximative theoretical description.

Concerning transition probabilities, experiment has been struggling to achieve error bars of less than a few per cent, even in favorable cases. However, theory for a long time has not tended to indicate even estimates of uncertainty, and eventually mismatches between experiment and theory have been found that—depending on the atomic system and the transition type—ranged from zero to factors of five or more. In the atomic system of present interest, we have concentrated on the five long-lived levels in the $n = 3$ shell. Measurements of the M1 transition rate in the ground term have reached an accuracy of well below 1%, a level at which the QED correction to the M1 transition operator plays a role. Without the EAMM correction to the M1 transition operator, our calculation is in agreement with the outcome of an experiment that carries an 0.7% error bar. If the estimate of a systematic error due to the 3s3p3d cascade even under the low-density conditions of an EBIT is applied to the former data, the agreement holds also for the QED-corrected lifetime. No

Table 16. Lifetime of the five long-lived levels among the lowest 40 levels of Al-like ions from K^{6+} to Ge^{19+}: $3s^23p\,^2P^o_{3/2}$, $3s3p^2\,^4P_{5/2,3/2,1/2}$ and $3s3p3d\,^4F^o_{9/2}$.

	$^2P^o_{3/2}$		$^4P_{5/2}$	$^4P_{3/2}$	$^4P_{1/2}$	$^4F^o_{9/2}$
Ion	Without QED correction to the M1 operator τ (ms)	With QED correction to the M1 operator τ (ms)	τ (ns)	τ (ns)	τ (ns)	τ (ms)
K^{6+}	3611	3595	2116	5719	1130	214.6
Ca^{7+}	1393	1387	1047	2941	574	142.2
Sc^{8+}	581.3	578.7	499	1517	250	97.62
Ti^{9+}	259.3	258.1	312	956	192	70.25
V^{10+}	122.2	121.7	182	586	117	50.83
Cr^{11+}	60.38	60.11	110	374	73.3	36.94
Mn^{12+}	31.11	30.97	69.0	247	47.5	26.67
Fe^{13+}	16.62	16.55	44.3	168	32.3	18.95
		16.74 ± 0.12[a]	39 ± 5[c]		29 ± 3[c]	
		$16.726 + 0.02 - 0.01$[b]				
Co^{14+}	9.172	9.131	29.2	118	21.5	13.18
			26 ± 1.5[c]		18 ± 1[c]	
Ni^{15+}	5.207	5.184	19.7	84.3	14.9	8.933
		5.27 ± 0.07[d]	16 ± 2[c]		12 ± 1.5[c]	10 ± 0.7[d]
Cu^{16+}	3.034	3.020	13.5	61.6	10.6	5.910
			10.5 ± 0.5[c]		8.5 ± 0.5[c]	
Zn^{17+}	1.810	1.802	9.50	45.9	7.61	3.831
			8.3 ± 0.6[c]		7.5 ± 1.0[c]	
Ga^{18+}	1.104	1.099	6.81	34.8	5.56	2.449
Ge^{19+}	0.6859	0.6828	4.98	26.9	4.13	1.552

[a] [68], [b] [70], [c] [25], [d] [72].

present calculation agrees with the result of a largely similar experiment that has been stated to carry a 0.1% error. For the lowest quartet levels and their spin-changing E1 decay, the agreement between theory and experiment (which is not very precise in this case) is reasonable; we note that measurements exist only for the $J = \frac{1}{2}$ and $\frac{5}{2}$ levels, whereas the longer-lived $J = \frac{3}{2}$ level remains unmeasured. For the 3s3p3d $J = \frac{9}{2}$ level, we present the first calculations for a series of elements. Cascade repopulation from this level has been invoked to explain a systematic shift of lifetime results at a heavy-ion storage ring from the results obtained at EBITs. In a single case, experiment has derived information on the cascade (in Al-like Ni), and the result is close to our prediction. In these measurements of long atomic lifetimes, experiment apparently will need further refinement before the actual level of validity of our calculations can be tested.

Acknowledgments

ET acknowledges travel support from the German Research Association (DFG). Part of this work has been performed at LLNL under the auspices of the USDoE under contract No. DE-AC52-07NA27344. YI acknowledges partial support from LLNL subcontracts No. B568401 and B579693. Work at the UPR was supported by the Fondo Institucional para la Investigacion (FIPI).

References

[1] Kim Y-K, Baik D H, Indelicato P and Desclaux J P 1991 *Phys. Rev.* A **44** 148
[2] Blundell S A 1993 *Phys. Rev.* A **47** 1790
[3] Froese Fischer C and Liu B 1986 *At. Data Nucl. Data Tables* **34** 261
[4] Gupta G P and Msezane A Z 2002 *Phys. Scr.* **66** 354
[5] Gupta G P and Msezane A Z 1999 *J. Phys. B: At. Mol. Opt. Phys.* **32** 3361
[6] Choudhury K B, Deb N C, Roy K and Msezane A Z 2003 *Eur. Phys. J.* D **27** 103
[7] Gupta G P and Msezane A Z 2004 *Phys. Scr.* **69** 273
[8] Gupta G P and Msezane A Z 2004 *Phys. Scr.* **70** 235
[9] Gupta G P and Msezane A Z 2007 *Phys. Scr.* **76** 225
[10] Gupta G P and Msezane A Z 2001 *J. Phys. B: At. Mol. Opt. Phys.* **34** 4217
[11] Gupta G P and Msezane A Z 2005 *At. Data Nucl. Data Tables* **89** 1
[12] Gupta G P and Msezane A Z 2008 *Eur. Phys. J.* D **49** 157
[13] Bhatia A K and Doschek G A 1999 *At. Data Nucl. Data Tables* **71** 69
[14] Deb N C and Msezane A Z 2001 *Phys. Scr.* **64** 212
[15] Gupta G P and Msezane A Z 2008 *Phys. Scr.* **77** 035303
[16] Farrag A, Luc-Koenig E and Sinzelle J 1982 *At. Data Nucl. Data Tables* **27** 539
[17] Fawcett B C 1983 *At. Data Nucl. Data Tables* **28** 557
[18] Huang K-N 1986 *At. Data Nucl. Data Tables* **34** 1
[19] Mendoza C, Eissner W, Le Dourneuf M and Zeippen C J 1995 *J. Phys. B: At. Mol. Opt. Phys.* **28** 3485
[20] Safronova U I, Namba C, Albritton J R, Johnson W R and Safronova M S 2002 *Phys. Rev.* A **65** 022507
[21] Safronova U I, Sataka M, Albritton J R, Johnson W R and Safronova M S 2003 *At. Data Nucl. Data Tables* **84** 1
[22] Fischer C F, Tachiev G and Irimia A 2006 *At. Data Nucl. Data Tables* **92** 607
[23] Wei H L, Zhang H, Ma C W, Zhang J Y and Cheng X L 2008 *Phys. Scr.* **77** 035301
[24] Träbert E, Hutton R and Martinson I 1987 *Z. Phys.* B **5** 125
[25] Träbert E, Heckmann P H, Hutton R and Martinson I 1988 *J. Opt. Soc. Am.* B **5** 2173

[26] Sugar J, Kaufman V and Rowan W L 1988 *J. Opt. Soc. Am.* B **5** 2183
[27] Redfors A and Litén U 1989 *J. Opt. Soc. Am.* B **6** 1447
[28] Ekberg J O, Redfors A, Brown C M, Feldman U and Seely J F 1991 *Phys. Scr.* **44** 539
[29] Raineri M, Bredice F, Gallardo M and Almandos J G R 1992 *Phys. Scr.* **45** 584
[30] Shirai T, Nakagaki T, Sugar J and Wiese W L 1992 *J. Phys. Chem. Ref. Data* **21** 273
[31] Shirai T, Nakai Y, Nakagaki T, Sugar J and Wiese W L 1993 *J. Phys. Chem. Ref. Data* **22** 1279
[32] Shirai T, Nakagaki T, Okazaki K, Sugar J and Wiese W L 1994 *J. Phys. Chem. Ref. Data* **23** 179
[33] Shirai T, Funatake Y, Mori K, Sugar J, Wiese W L and Nakai Y 1990 *J. Phys. Chem. Ref. Data* **19** 127
[34] Shirai T, Mengoni A, Nakai Y, Sugar J, Wiese W L, Mori K and Sakai H 1992 *J. Phys. Chem. Ref. Data* **21** 23
[35] Shirai T, Mori K, Sugar J, Wiese W L, Nakai Y and Ozawa K 1987 *At. Data Nucl. Data Tables* **37** 235
[36] Shirai T, Nakagaki T, Nakai Y, Sugar J, Ishii K and Mori K 1991 *J. Phys. Chem. Ref. Data* **20** 1
[37] Shirai T, Reader J, Kramida A E and Sugar J 2007 *J. Phys. Chem. Ref. Data* **36** 509
[38] Shirai T, Nakai Y, Ozawa K, Ishii K, Sugar J and Mori K 1987 *J. Phys. Chem. Ref. Data* **16** 327
[39] Shirai T, Okazaki K and Sugar J 1995 *J. Phys. Chem. Ref. Data* **24** 1577
[40] Shirai T, Sugar J, Musgrove A and Wiese W L 2000 *Spectral data for Highly Ionized Atoms: Ti, V, Cr, Mn, Fe, Co, Ni, Cu, Kr, and Mo* Monograph No. 8 (Melville, NY: AIP) Isbn 1-56396-934-3
[41] Träbert E *et al* 1993 *Phys. Rev.* A **47** 3805
[42] Hutton R 1997 *Phys. Scr.* T **73** 25
[43] Bengtsson P, Ando K, Kambara T, Awaya Y and Hutton R 1997 *Phys. Scr.* T **73** 81
[44] Träbert E, Staude U, Bosselmann P, Schartner K H, Mokler P H and Tordoir X 1998 *Eur. Phys. J.* D **2** 117
[45] Vilkas M J, Ishikawa Y and Träbert E 2006 *Eur. Phys. J.* D **41** 77
[46] Redfors A and Litzén U 1988 *Phys. Lett.* A **127** 88
[47] Jupén C and Curtis L J 1996 *Phys. Scr.* **53** 312
[48] Träbert E, Wagner C, Heckmann P H, Möller G and Brage T 1993 *Phys. Scr.* **48** 593
[49] Churilov S S and Levashov V E 1993 *Phys. Scr.* **48** 425
[50] Møller C and Plesset M S 1934 *Phys. Rev.* **46** 618
[51] Vilkas M J and Ishikawa Y 2005 *Phys. Rev.* A **72** 032512
[52] Vilkas M J and Ishikawa Y 2003 *Phys. Rev.* A **68** 012503
[53] Ralchenko Yu, Jou F-C, Kelleher D E, Kramida A E, Musgrove A, Reader J, Wiese W L and Olsen K 2005 *NIST Atomic Spectra Database (Version 3.0.2)* Available online at http://physics.nist.gov/asd3 (Gaithersburg, MD: National Institute of Standards and Technology)
[54] Engström L, Kirm M, Bengtsson P, Maniak S T, Curtis L J, Träbert E, Doerfert J and Granzow J 1995 *Phys. Scr.* **52** 516
[55] Cowan R D 1981 *The Theory of Atomic Structure and Spectra* (Berkeley, CA: University of California Press)
[56] Vilkas M J, Ishikawa Y and Träbert E 2006 *J. Phys. B: At. Mol. Opt. Phys.* **39** 2195
[57] Vilkas M J and Ishikawa Y 2002 *Phys. Scr.* **65** 219
[58] Vilkas M J and Ishikawa Y 2003 *J. Phys. B: At. Mol. Opt. Phys.* **36** 4641
[59] Vilkas M J and Ishikawa Y 2004 *J. Phys. B: At. Mol. Opt. Phys.* **37** 1803
[60] Vilkas M J and Ishikawa Y 2004 *J. Phys. B: At. Mol. Opt. Phys.* **37** 4763
[61] Vilkas M J and Ishikawa Y 2004 *Phys. Rev.* A **69** 062503
[62] Vilkas M J, Ishikawa Y and Träbert E 2005 *Phys. Scr.* **72** 181
[63] Vilkas M J, Ishikawa Y and Koc K 1998 *Phys. Rev.* E **58** 5096
[64] Ishikawa Y, Koc K and Schwarz W H E 1997 *Chem. Phys.* **225** 239
[65] Ishikawa Y, Quiney H M and Malli G L 1991 *Phys. Rev.* A **43** 3270
[66] Indelicato P, Gorceix O and Desclaux J P 1987 *J. Phys. B: At. Mol. Opt. Phys.* **20** 651
[67] Träbert E 2004 *Astron. Astrophys.* **415** L39
[68] Beiersdorfer P, Träbert E and Pinnington E H 2003 *Astrophys. J.* **587** 836
[69] Lapierre A *et al* 2006 *Phys. Rev.* A **73** 052507
[70] Brenner G, Crespo López-Urrutia J R, Harman Z, Mokler P H and Ullrich J 2007 *Phys. Rev.* A **75** 032504
[71] Calamai A G, Smith P L and Bergeson S D 1993 *Astrophys. J.* **415** L59
[72] Träbert E, Hoffmann J, Krantz C, Wolf A, Ishikawa Y and Santana J A 2009 *J. Phys. B: At. Mol. Opt. Phys.* **42** 025002
[73] Krueger T K and Czyzak S J 1966 *Astroph. J.* **144** 1194
Krueger T K and Czyzak S J 1967 *Astroph. J.* **149** 237 (erratum)
[74] Warner B 1968 *Z. Astrophys.* **69** 399
[75] Smith M W and Wiese W L 1973 *J. Phys. Chem. Ref. Data* **2** 85
[76] Kastner S O 1976 *Sol. Phys.* **46** 179
[77] Kafatos M and Lynch J P 1980 *Astroph. J. Suppl.* **42** 611
[78] Eidelsberg M, Crifo-Magnant F and Zeippen C J 1981 *Astron. Astroph. Suppl.* **43** 455
[79] Kaufman V and Sugar J 1986 *J. Phys. Chem. Ref. Data* **15** 321
[80] Biémont E, Cowan R D and Hansen J E 1988 *Phys. Scr.* **37** 850
[81] Bhatia A K and Kastner S O 1993 *J. Quant. Spectrosc. Radiat. Transfer* **49** 609
[82] Moehs D P and Church D A 1999 *Astroph. J.* **516** L111
[83] Storey P J, Mason H E and Young P R 2000 *Astron. Astrophys. Suppl. Ser.* **141** 285
[84] Smith S J, Chutjian A and Lozano J A 2005 *Phys. Rev.* A **72** 062504
[85] Träbert E, Gwinner G, Wolf A, Knystautas E J, Garnir H-P and Tordoir X 2002 *J. Phys. B: At. Mol. Opt. Phys.* **35** 671
[86] Träbert E 2008 *Can. J. Phys.* **86** 73